Placental adaptation to early-onset hypoxic pregnancy and mitochondria-targeted antioxidant therapy in the rat

Anna Maria Nuzzo[1]*, Emily J. Camm[2,4]*, Amanda N. Sferruzzi-Perri[2,4], Thomas J. Ashmore[2#], Hong-wa Yung[2,4], Tereza Cindrova-Davies[2,4], Ana-Mishel Spiroski[2#], Megan R. Sutherland R[2#], Angela Logan [3], Shani Austin-Williams[2#], Graham J. Burton[2,4], Alessandro Rolfo[1], Tullia Todros[1], Michael P. Murphy[3] and Dino A. Giussani[2,4]

[1]Department of Surgical Sciences, University of Turin, Italy; [2]Department of Physiology, Development & Neuroscience, University of Cambridge, Cambridge, United Kingdom; [3]MRC Mitochondrial Biology Unit, University of Cambridge, United Kingdom; [4]Centre for Trophoblast Research, Cambridge, United Kingdom.

Number of text pages: 35

Number of figures: 8

Number of tables: 2

Running title: Placental adaptation to hypoxia and MitoQ

Grant funding: British Heart Foundation (grant number: PG/14/5/30547). Work in MPM's Laboratory is supported by the Medical Research Council UK (MC_U105663142) and by a Wellcome Trust Investigator award (110159/Z/15/Z). ANS-P is supported by a Royal Society Dorothy Hodgkin Research Fellowship.

Correspondence: Professor Dino A. Giussani

Department of Physiology, Development & Neuroscience

University of Cambridge, Cambridge, CB2 3EG, UK

Tel: +44 1223 333816

Fax: +44 1223 333840

E-mail: dag26@cam.ac.uk

*AMN and EJC contributed equally as first authors

#Current addresses: AMS, Queen's Medical Research Institute, University of Edinburgh, United Kingdom; MRS, Department of Anatomy and Developmental Biology, Monash University, Australia; TJA, University of Cambridge Metabolic Research Laboratories, Institute of Metabolic Science, Cambridge, United Kingdom; SA-W., William Harvey Research Institute, Queen Mary University of London, United Kingdom.

ABSTRACT

The placenta responds to adverse environmental conditions by adapting its capacity for substrate transfer to maintain fetal growth and development. The effects of early-onset hypoxia on placental morphology and activation of the unfolded protein response (UPR) were determined using an established rat model in which fetal growth restriction is minimised. We further established whether maternal treatment with the mitochondria-targeted antioxidant (MitoQ) confers protection during hypoxic pregnancy. Wistar dams were exposed to normoxia (N, 21% O_2) or hypoxia (H, 13-14% O_2) from days 6-20 of pregnancy with and without MitoQ treatment (500 µM in drinking water). On day 20, animals were euthanased and weighed, and the placentae from male fetuses were processed for stereology to assess morphology. Western blotting was used to determine activation of the UPR in additional cohorts of frozen placentae. Neither hypoxic pregnancy nor MitoQ treatment affected fetal growth. Hypoxia increased placental volume and the fetal capillary surface area within the labyrinthine transport zone, induced mitochondrial stress as well as the UPR as evidenced by upregulation of GRP78 and ATF4 protein abundance. Treatment with MitoQ in hypoxic pregnancy increased placental maternal blood space surface area and volume and prevented the activation mitochondrial stress and ATF4 pathway. The data suggest that mitochondria-targeted antioxidants may be beneficial in complicated pregnancy via mechanisms protecting against placental stress and enhancing placental perfusion.

Abbreviations: 4-HNE: 4-Hydroxynonenal; AKT: Protein kinase B; ATF4: activating transcription factor 4; ATF6: activating transcription factor 6; CAST: The Computer Assisted Stereology Toolbox; DB: decidua basalis; Dvm: diffusing capacity; ER: endoplasmic reticulum; FC: fetal capillaries; GRP75: glucose-regulated protein 75; GRP78: glucose-regulated protein 78; H: hypoxia; HM: hypoxia with MitoQ; HSP70: 70kDa heat-shock protein; IRE1: inositol-requiring enzyme; IUGR: intrauterine growth restriction; JZ: junctional zone; LC-MS/MS: liquid chromatography tandem mass spectrometry; LZ: labyrinthine zone; LIM: labyrinthine zone interhaemal membrane K: Krogh diffusion coefficient for oxygen; MBS: maternal blood spaces; MitoQ: mitochondrial-targeted antioxidant; N: normoxia; NM: normoxia with MitoQ: PERK: protein kinase RNA (PKR)-like ER kinase; P-AKT (Thr308): phosphorylated Protein kinase B; ROS: reactive oxygen species; SDC: Specific Diffusion Capacity TDC: Theoretical Diffusion Capacity; Th: thickness; TID-1: tumorous imaginal disc 1; UPR: unfolded protein response.

INTRODUCTION

The placenta is the main interface between the mother and fetus, and regulates intrauterine development by supplying nutrients and oxygen required for fetal growth. There is now clear evidence that the placenta is able to sense and respond to supply signals arising from the mother, and demand signals from the fetus. The organ can adapt morphologically and functionally to these signals, for instance, by altering placental and fetal blood flow, fetal nutrient supply and secretion of signalling molecules, including hormones [1]. To date, the majority of the research effort on placental adaptation to adverse pregnancy has focussed on maternal nutritional challenges, or maternal glucocorticoid over-exposure, and their effects on placental structure and function [2, 3]. Chronic fetal hypoxia is one of the most common consequences of complicated pregnancy, and is associated with a variety of maternal, placental, and fetal conditions, including pregnancy at high-altitude, gestational diabetes, preeclampsia and placental insufficiency [4, 5]. Despite this, the effect of hypoxia on the placenta remains relatively unexplored. Decrements in fetal growth have been observed in rodents exposed to hypoxia during mid to late pregnancy [6-8]. Interestingly, compared with late-onset hypoxic pregnancy that restricts fetal growth [8-10], hypoxia exposure earlier in pregnancy does not necessarily reduce fetal or birth weight [11, 12]. This suggests that there are adaptations in materno-fetal resource allocation during early-onset hypoxia that help to maintain fetal growth and appropriate development. In relation to the effects of hypoxic pregnancy on placental morphology, the available data from studies in rodents are variable. Increases, decreases or no difference in placental weights, the surface area and volumes of the maternal and/or fetal compartments, barrier thickness, and transfer of glucose and amino acids and their transporters, have been reported [7, 13-17]. This variability is most likely due to differences in the duration, severity, and mode of induction, and whether exposure to hypoxia is accompanied by reductions in maternal food intake during the challenge [9, 12, 18, 19].

Placental oxidative stress is implicated in the pathophysiology of several complications of human pregnancy, including preeclampsia [20, 21], high-altitude pregnancy [22, 23], and cases of intrauterine growth

restriction (IUGR) [24]. Closely associated to oxidative stress is disruption of endoplasmic reticulum (ER) function. The ER is a site of integration of various stress responses, including hypoxia, mediated principally through the unfolded protein response (UPR), which aims to restore normal ER function [25-27]. The UPR comprises three highly conserved parallel signalling branches: protein kinase RNA (PKR)-like ER kinase (PERK), inositol-requiring enzyme (IRE1) and activating transcription factor 6α (ATF6). Activation of these pathways have been reported in placentae from human IUGR infants with or without preeclampsia [28-30], and to a lesser extent in healthy pregnancies at high-altitude [23].

Recently, the potential use of antioxidant therapies to protect the placenta and fetus against oxidative stress in complications of pregnancy and birth has attracted much attention. We developed a rodent animal model of hypoxic pregnancy that minimises effects on maternal food intake, thereby helping to isolate the effects of hypoxia on the placenta and offspring [11, 31]. Using this model, we have shown that early-onset hypoxia from days 6-20 of gestation increases placental size and induces placental oxidative stress, and that maternal treatment with the antioxidant vitamin C is protective [11, 31, 32]. While these data provide proof-of-principle that maternal antioxidant therapy may confer protection to the placenta and offspring in hypoxic pregnancy, in these studies only high doses of vitamin C were effective. In addition, clinical trials have reported that maternal treatment with vitamin C in human pregnancy complicated by preeclampsia did not prove protective to the mother or baby [33, 34]. Therefore, there is increasing interest in alternative maternal antioxidant therapies to protect the placenta and offspring in complicated pregnancy with greater translational capacity to the human clinical situation.

Mitochondria-targeted antioxidants might offer a plausible alternative, as the majority of endogenous reactive oxygen species (ROS) are generated within mitochondria [35]. The most extensively studied compound of this class is the mitochondria-targeted ubiquinone derivative MitoQ, which can pass easily

through all biological membranes and accumulate several-hundred fold within mitochondria, thereby enhancing protection from oxidative damage [36, 37]. The use of MitoQ *in vivo* in several different rodent models of human pathology, has shown that MitoQ can protect against oxidative damage in adult offspring [38-45]. Further, long-term oral administration is safe, and unlike other conventional antioxidants, MitoQ does not demonstrate pro-oxidant activity at high doses *in vivo* [46, 47]. An oral preparation of MitoQ has already safely undergone Phase I and II human clinical trials. A study demonstrated that MitoQ can be safely administered for one year and is well tolerated by patients [48]. To date, only one study has investigated the antioxidant benefits of MitoQ in pregnancy, reporting that treatment of the pregnant rat with nano-particle bound MitoQ during hypoxic pregnancy could protect fetal brain development [49]. Therefore, the aim of this study was to investigate the effects of hypoxic pregnancy with and without maternal treatment with MitoQ on placental morphological capacity for substrate transport, and to determine whether UPR-sensing mechanisms were affected.

MATERIALS AND METHODS

Experimental design

All procedures described were approved by the Ethical Review Committee of the University of Cambridge, and were in accordance with UK Animals (Scientific Procedures) Act 1986. Power calculations derived from previously published data using a similar experimental design [11, 31, 50] were used to determine the minimum numbers required for statistically valid results taking into account, sex of the offspring and variations in litter size. Virgin Wistar rats (Charles River, UK; 10-12 weeks of age) were mated with male Wistar rats (minimum 12 weeks of age) overnight. Pregnancy was confirmed by the presence of a copulatory plug (day 0, term ~22 days). Pregnant dams were then housed individually (21°C, 60% humidity, 12 h: 12 h light–dark cycle) with free access to food (Special Diet Services, UK) and water. Maternal weight, food and water consumption were monitored daily throughout gestation. On day 6 of pregnancy, rats were randomly assigned to either normoxic (21% O_2) or hypoxic (13%-14% O_2) conditions. Two additional normoxic and hypoxic groups were examined, and were given the mitochondria-targeted antioxidant MitoQ (500 µM in maternal drinking water), which was prepared fresh daily. Pregnant dams subjected to hypoxia were placed inside a chamber, which combined a PVC isolator with a nitrogen generator, as previously described [31, 32, 51]. The experimental design therefore consisted of four groups: normoxia (N, n=16 litters), hypoxia (H, n=16 litters), hypoxia with MitoQ (HM, n=18 litters) and normoxia with MitoQ supplementation (NM, n=16 litters). The dose of MitoQ was derived from previous animal studies [39, 46, 47, 52], and corresponds to an oral dose of ~0.05 mg/d/g in rats [38].

Tissue Collection

On day 20 of gestation, all dams underwent euthanasia by CO_2 inhalation and cervical dislocation. A maternal blood sample for measurement of haematocrit was taken by cardiac puncture. The pregnant

uterus was exposed via a mid-line incision and the pups killed via spinal transection. Maternal blood was centrifuged for determination of haematocrit. All fetuses and their associated placentae were weighed. To control for within-litter variation, one placenta was randomly selected and processed for stereology. Another two placentae from each litter were collected and immediately frozen in liquid nitrogen for MitoQ uptake and protein isolation analyses, respectively. Therefore, only 1 placenta per litter was used for each outcome measure. Only placentae from male pups were collected, to control for sex variation.

MitoQ Uptake

The uptake of MitoQ was assessed in the placenta, maternal liver and fetal liver. MitoQ was measured using a liquid chromatography tandem mass spectrometry (LC-MS/MS) assay [46]. Frozen tissues were homogenised in Tris buffer (pH 7.0) and extracted with acetonitrile (Sigma-Aldrich, UK) and dried overnight under a vacuum. The extracts were reconstituted and the MitoQ content measured using mass spectrometry. Data were analysed using MassLynx MS software (Waters, UK), and expressed relative to a deuterated internal standard. Control samples were spiked with known amounts of MitoQ from 1 to 500pmol in order to generate a standard curve; the assay could detect as low as 0.1pmol MitoQ/100mg of tissue.

Placental histology and stereology

At post-mortem, the placentae randomly selected for stereology were transversally cut into two halves. One half was immersion fixed in 4% paraformaldehyde (4% PFA), embedded in paraffin wax, then completely sectioned at 7 µm perpendicular to the chorionic plate (Leica RM 2235 microtome, Leica Microsystems, Germany). Systematic random sampling was used to select, without bias, 10 sections for analysis [53]. Haematoxylin and eosin (H&E) staining of these sections was used to visualise the gross structure of the rat placenta. Immunohistochemistry was performed on sections near the placental

midline for markers of mitochondrial stress (glucose-regulated protein 75 [GRP75] and tumorous imaginal disc 1 [TID-1]), and to localise activating transcription factor 4 (ATF4) and glucose-regulated protein 78 (GRP78). The other half of the placenta was fixed with 4% glutaraldehyde and embedded in Spurr epoxy resin. A 1 μm thick section was cut near to the placental midline and stained with toluidine blue to visualise the structure of the labyrinthine zone [54].

The Computer Assisted Stereology Toolbox (CAST) 2.0 system from Olympus (Ballerup, Denmark) fitted with a motorised specimen stage was used to perform all stereological measurements. All quantitative analyses were performed with the observer blind to the treatment group. To determine the absolute volume of the placenta, a point grid was superimposed on vertically orientated H&E-stained paraffin sections viewed using a x1.25 objective lens. Points falling on the sample were counted and the Cavalieri principle was applied in order to reach a volume estimate [55]:

$$V(obj) = t \times \Sigma a = t \times a(p) \times \Sigma P$$

where $V_{(obj)}$ is the estimated placental volume, t is the total thickness of the placenta (total number of sections multiplied by section thickness), $a_{(p)}$ is the area associated with each point, and Σ P is the sum of points on sections. At ×10 magnification, meander sampling and point counting was employed to estimate compartment densities of the three placental zones: labyrinthine zone (LZ), junctional zone (JZ) and decidua basalis (DB):

$$Vv\ (struct,ref) = P\ (struct) / P\ (total)$$

where Vv (struct,ref) is the volume fraction of a compartment (e.g. LZ) within a reference space (e.g. placenta), P(struct) is the number of points falling on the compartment, and P(total) is the total number of points falling on the reference space (including the component). The volume densities obtained were converted to absolute quantities by multiplying by total placental volume [55, 56].

Resin sections were used to resolve the labyrinth structure in detail. A x100 objective lens was used, and fields of view within the LZ were selected by meander sampling to determine volume densities, surface densities and interhaemal membrane thickness. Volume densities of the maternal blood space (MBS) and fetal capillaries (FC) were obtained using a point grid [54]. Volume densities were converted to absolute component volumes by multiplying by the volume of the LZ. Vascular surface densities for the MBS and FC were obtained using a grid formed of cycloid arcs placed over each field of view and intercepts between maternal blood space boundary and fetal capillary boundary were counted. The following equation was used to determine surface areas:

$$S(struct) = (2 \times \Sigma I(struct) / I(p) \times \Sigma P(ref)) \times V(ref)$$

where $\Sigma I(struct)$ is the total number of intersections of the cycloid arcs with the structure, $\Sigma P(ref)$ is the total number of points that hit the reference space, and I(p) is the length of the test line associated with each point in the grid [57]. All surface area densities were converted to absolute surface areas by multiplying by the volume of LZ. Thickness of the interhaemal membrane of the LZ was obtained with a line grid to establish random start points for measuring distances between FC and the closest MBC by the method of orthogonal intercepts [58]. Intercept lengths were multiplied by the factor $(8/3)\pi$ to correct for plane of sectioning [59], and the harmonic mean thickness (Th) of the membrane calculated as the reciprocal of the mean of the reciprocals of the corrected intercept distances. The Theoretical Diffusion Capacity (TDC) for the interhaemal membrane was calculated using the equation:

$$Dvm = K \times (\text{mean surface area}/Th)$$

where Dvm is the diffusing capacity across the LZ membrane, K is the Krogh diffusion coefficient for oxygen (17.3×10^{-8} cm^2 min^{-1} kPa^{-1}) [60], mean surface area is the mean of fetal and maternal surface areas of the Interhaemal Membrane (LIM), and Th is the harmonic mean thickness of the LIM. The Specific Diffusion Capacity (SDC) is an estimate of the diffusing capacity for oxygen in terms of fetal requirements, obtained by expressing Dvm per mg of fetal weight.

Immunohistochemistry

Sections near the placental midline were dewaxed then rehydrated in water for 10 minutes, incubated with 3% H_2O_2 for 15 minutes, washed in tap water before antigen retrieval was performed (Tris-EDTA buffer, pH 9.0; Sigma-Aldrich, UK). Sections were washed with Tris-buffered saline with 1% Triton-X and 1% Tween-20 (TBS-TT; all Sigma-Aldrich, UK) for 30 minutes then specific binding was blocked with 5% BSA in TBS (Sigma-Aldrich, UK) for 1 hour. Sections were then incubated overnight at 4°C with the following primary antibodies: UPR-related proteins anti-GRP78 (1:1000; Transduction Laboratories, BD Biosciences, UK) and anti-ATF4 (1:250; Santa Cruz Biotechnology, UK), as well as markers of the mitochondrial matrix anti-TID-1 (1:100; GeneTex, UK) and anti-GRP75 (1:100; Abcam, UK). Negative control samples were obtained by omitting the primary antibody. The following day, sections were washed 15 minutes in TBS-TT, incubated for 1 hour with secondary antibody (Vector Laboratories, U.S.A.) then washed for 15 minutes in TBS-TT. Sections were incubated for 45 minutes in Avidin/Biotin (AB; Vector Laboratories, UK) in TBS, then washed in TBS for 10 minutes. Staining was visualized with DAB/H_2O_2 (Sigma-Aldrich, UK) for 2 minutes. Slides were rinsed with water, dehydrated and then cover slipped with DPX (Sigma-Aldrich, UK).

Optical Density

Optical density (OD) of GRP75 and TID-1 immunostaining was measured in the LZ and JZ using a calibrated optical density step tablet (ImageJ V1.80, National Institutes of Health). For each placenta, ten fields within each region (LZ and JZ) were examined.

Western blot analysis

Whole placental tissue was homogenised in cell lysis buffer and a mini proteases inhibitor cocktail (Roche Diagnostics, East Sussex, UK). The protein concentration of the lysates was measured by a bicinchoninic acid protein assay (BCA, Sigma-Aldrich, UK). The samples were mixed with SDS-PAGE gel loading buffer (50 mM Tris-HCl, pH 6.8, 100 mM dithiothreitol, 2% SDS, 10% glycerol, bromophenol blue) and boiled for 5 minutes. Equivalent amounts of protein (1 µg/µl) were resolved by SDS-PAGE, blotted onto nitrocellulose membranes (0.2 µm), and probed overnight at 4°C with the following primary antibodies: anti-GRP78 (Transduction Laboratories, BD Biosciences, UK), anti-protein kinase B (AKT, Cell Signaling Technology, UK), anti-ATF-4 (Santa Cruz Biotechnology, UK), anti-phosphorylated protein kinase B (Thr308) (p-AKT, Santa Cruz Biotechnology, UK), anti-4-hydroxynonenal (4-HNE, Merck Millipore, UK) and anti-70kDa heat-shock protein (HSP70, Enzo Life Sciences, UK). Anti-β-actin (Sigma-Aldrich, UK) was used to normalise protein levels. Some membranes were re-probed with antibodies of different molecular weight or those which were raised in a different species. The membranes were analysed by enhanced chemiluminescence (ECL, Amersham Biosciences, UK) using Kodak X-OMAT androgen receptor (AR) film (Sigma-Aldrich, UK). Films were scanned using a flat-bed scanner (Cannon 8000F) and the intensity of the bands were determined from two or three different exposures (within the linear detection range) using ImageJ analysis software [61].

Statistical Analyses

All data are expressed as mean ± S.E.M. Maternal pregnancy variables and biometry, placenta stereology and molecular analyses were compared statistically using a General Linear Model (GLM) test with repeated measures when appropriate (IBM SPSS V24.0). Fetal biometry was assessed using the Linear Mixed Models (IBM SPSS V24.0), which nests offspring data within a maternal identifier, thereby

accounting for the shared maternal environment [62]. For all comparisons, significance was accepted when $p<0.05$.

RESULTS

Maternal and fetal biometry

Maternal hypoxia induced a significant increase in maternal haematocrit (Table 1, p=0.002) and placental weight (Table 2, p=0.002). Body weight and other fetal biometric variables were unaltered by hypoxic pregnancy or MitoQ treatment (Table 2, p>0.05). Similarly, litter size (N: 15.3±0.8; H: 16.8±0.6; HM: 14.5±1.0; NM: 14.00±1.2) and sex ratio (percentage of males N: 49.5±4.0%; H: 50.6 ±3.4%; HM: 54.5±4.9%; NM: 46.1±3.8%) were unchanged (both p>0.05). Maternal exposure to hypoxia did not alter maternal weight gain with advancing gestation, nor reduce maternal food or water intake until days 18 of gestation (Figure. 1A-C). Between days 18-19 of gestation, all pregnant dams showed a reduction in maternal food intake relative to days 7-17 of gestation (all p<0.05), which was more pronounced in hypoxic relative to normoxic pregnancy (Figure 1B, p=0.002). Maternal treatment with MitoQ in normoxic and hypoxic pregnancy led to a transient but significant fall of similar magnitude in maternal food and water intake (Figure 1A,B) and maternal body weight (Figure 1C) soon after the onset of administration on day 6 of gestation (all p≤0.001). Shortly afterwards maternal body weight gain, and food and water intake recovered towards control values with advancing gestation in normoxic and hypoxic pregnancy treated with MitoQ. However, in MitoQ-treated pregnancies, water rather than food intake, appeared more affected (Figure 1).

MitoQ uptake

MitoQ uptake (pmol MitoQ/g wet weight of tissue), measured by a liquid chromatography tandem mass spectrometry assay, was expressed relative to untreated normoxic and hypoxic dams and their fetuses. By day 20 of gestation, MitoQ accumulation was greatest in the maternal liver (HM: 173±37pmol/g, n=9; NM: 192±40pmol/g, n=10), followed by the placenta (HM: 132±28pmol/g, n=10; NM: 78±24pmol/g, n=11), and then fetal liver (HM: 8.5±2.2pmol/g, n=10; NM: 11.4±3.7pmol/g, n=10).

Placental morphology

At day 20 of gestation, the absolute volume of hypoxic placentae was greater than that of normoxic placentae (Figure 2A, p=0.014). The absolute volumes of the labyrinthine zone, junctional zone and decidua were proportionally increased in hypoxic pregnancies (Figure 2B, LZ: p=0.046; JZ: p=0.034; DB: p=0.015). While hypoxia did not affect total fetal capillary volume in the labyrinthine zone (Figure 3A, p>0.05), total fetal capillary surface area was significantly increased compared to normoxic placentae (Figure 3B, p=0.005); maternal blood space volume and surface area were unchanged (Figure 3D, both p>0.05). Placental efficiency, expressed as the ratio of fetal body weight to fetal capillary area and maternal blood space area was significantly reduced in placentae from hypoxic pregnancy (Figure 4, p=0.021). Interhaemal membrane thickness, theoretical and specific diffusion capacity were unaltered in hypoxic pregnancy (Figure 5A-C, all p>0.05).

In hypoxic pregnancy treated with MitoQ, absolute placenta volume was increased relative to normoxic pregnancy (Figure 2A, p=0.039). Further, the absolute volume of the decidua basalis was increased (Figure 2B, p=0.010). MitoQ treatment in hypoxic pregnancy did not alter absolute fetal capillary volume (Figure 3A, p>0.05); however, fetal capillary surface area was increased relative to placentae from normoxic pregnancy (Figure 3B, p=0.049). In addition, MitoQ treatment in hypoxic pregnancy increased both maternal blood space volume (Figure 3C, p=0.033) and surface area (Figure 3D, 0.041). Placental efficiency (Figure 4), the thicknesses of the interhaemal membrane, and the theoretical and specific diffusion capacities remained unaltered (Figure 5A-C, all p>0.05). In normoxic pregnancy, MitoQ administration did not affect placental morphology (Figures 2-5, all p>0.05).

Placental unfolded protein response, cell proliferation and oxidative and mitochondrial stress signalling pathways

In hypoxic pregnancy, GRP78 (Figure 6A, p=0.001) and ATF4 abundance (Figure 6B, p<0.001) were significantly increased in the placenta relative to normoxic pregnancy. In hypoxic pregnancy treated with MitoQ, GRP78 remained elevated relative to normoxic pregnancies (Figure 6A, p=0.032); however, ATF4 expression was restored to normoxic levels (Figure 6B, p=0.130). There was no effect of MitoQ supplementation in normoxic pregnancy on GRP78 or ATF4 (Figure 6A-D, both p>0.05). Across all treatment groups, GRP78 expression was localised to the JZ, while AFT4 staining was seen in both the LZ and JZ (Figure 6). Total AKT (Figure 7A), p-AKT (Thr 308) (Figure 7B), HSP70 (Figure 7C) and 4-HNE (Figure 7D) were unaltered by hypoxia and/or MitoQ (all p>0.05).

Both GRP75 and TID-1, which localise to the mitochondrial matrix, were ubiquitously expressed throughout the placenta. The staining intensity (optical density, OD) of GRP75 was increased in both the LZ (Figure 8A) and JZ (N: 0.23±0.1; H: 0.29±0.02; HM: 0.24±0.01; NM: 0.21±0.01, both p<0.05) in hypoxic placentae, but restored with MitoQ treatment. A similar trend was observed with TID-1, which was increased in the LZ in hypoxic pregnancy only (Figure 8B). No changes in TID-1 staining were observed in the JZ (N: 0.18±0.1 O.D.; H: 0.20±0.01; HM: 0.16±0.02; NM: 0.16±0.01, all p>0.05). There was no effect of MitoQ supplementation in normoxic pregnancy on GRP75 or TID-1 staining (Figure 8A,B, both p>0.05).

DISCUSSION

The data show that early-onset hypoxic pregnancy modifies the placental morphological phenotype which offsets increased signalling in placental UPR pathways to maintain fetal growth. Hypoxic pregnancy increased placental volume and the fetal capillary surface area within the labyrinthine transport zone and induced the UPR and mitochondrial stress, as evidenced by upregulation of GRP78, ATF4, GRP75 and TID-1 protein abundance. Maternal treatment with the mitochondria-targeted antioxidant MitoQ in hypoxic pregnancy further increased placental maternal blood space surface area and volume, and restored activation of the ATF4 pathway, normalising UPR and mitochondrial stress signalling mechanisms towards levels observed in normoxic pregnancy.

Effects of hypoxic pregnancy on placental morphology and fetal biometry

In the rat, the placenta is fully developed by around day 14 of gestation [63]. This means that in the present model of hypoxic pregnancy, the placenta developed under hypoxic conditions. In our study, we demonstrate that the placenta adapts morphologically to early-onset hypoxia by increasing placental volume. Volumes of the decidua basalis, junctional zone and labyrinthine zone were proportionally larger in hypoxic pregnancy, in association with expansion of the fetal capillary surface area within the labyrinthine zone. No changes were observed in the volume or surface area of maternal blood spaces, or thickness of the placental interhaemel membrane. Similar beneficial changes in placental vascularisation have been observed in the placentae of mice (13% oxygen, d1-19 [15] and d14-19 [13]) and rats (11% oxygen, d7-14, [16, 17]) exposed to hypoxia from early to mid-pregnancy, and in human pregnancy at high altitude [56, 64]. The increase in fetal capillary blood surface area may represent a compensatory adaptation to increase or maintain placental transport capacity, thereby protecting fetal growth. By contrast, hypoxic pregnancy treated with MitoQ not only increased placental volume and fetal capillary surface area in the labyrinthine zone, but also expanded maternal blood spaces. The thickness of the placental interhaemel membrane

was not altered. The ability of MitoQ to enhance maternal blood perfusion of the hypoxic placenta may represent an additional protective mechanism to enhance the delivery of substrates for fetal growth. Accordingly, data in the present study also show that maternal treatment with MitoQ in hypoxic pregnancy also restored the impaired placental efficiency to control levels. Nitric oxide (NO) is important for the maintenance of umbilical blood flow; an increase in NO bioavailability can promote umbilical vasodilatation. We have previously shown that the antioxidants melatonin and vitamin C can increase umbilical blood flow via nitric oxide-dependent mechanisms [65]. MitoQ has been shown to improve endothelial function in aged mice [66] and stroke-prone spontaneously hypertensive (SHRSP) rats [39], by enhancing NO bioavailability. Substantial evidence suggests that endothelium-derived NO is a major mediator of angiogenesis [67]. Taken together, these lines of evidence suggest that the enhanced volume of maternal blood spaces in the placenta of MitoQ-treated hypoxic pregnancies may be secondary to an increase in NO availability and NO-induced angiogenesis of uterine vessels that supply the labyrinthine zone.

Effects of hypoxic pregnancy on unfolded protein response and cell proliferation signalling mechanisms

There are three arms of the UPR signalling pathway, including PERK, ATF6 and IRE1. Our previous publications have demonstrated only activation of the PERK-eIF2α-ATF4 arm of the pathway in mice housed under hypoxic conditions [15], in human placentas from high altitude [23] and in trophoblast cells exposed to 1% O_2 [23]. Therefore, we decided to focus on the PERK arm of the UPR signalling pathway. ATF4 expression is a known readout of the phosphorylation status of eIF2α. We have previously reported activation of eIF2α when tissue was collected 30 minutes following placental separation from the uterine wall [68]. In comparison to the process of phosphorylation which rapidly switches on and off, the expression of the ATF4 gene and then translation into proteins takes considerably longer and is less influenced by tissue collection and handling. Therefore, we considered ATF4 as biomarker for ER stress in the present study. GRP78 protein abundance was shown to be increased in the placenta of hypoxic pregnancy, with

or without MitoQ treatment. In addition, ATF4 protein abundance was significantly elevated in hypoxic pregnancy, but restored to normoxic levels with MitoQ treatment. GRP78, an ER chaperone protein, plays a crucial role in the regulation of the ER dynamic equilibrium and guides misfolded proteins out of the ER and into the cytosol for degradation [69]. PERK-ATF4 is a key UPR signalling mechanism in the adaptive response of cells to oxidants, and increases in response to cellular stresses [70]. Under hypoxic conditions, there is not only an increase in mitochondrial ROS production, but also a disruption of calcium homeostasis in the mitochondria, cytosol and ER [71]. Loss of calcium from the ER lumen, which leads to a perturbation in ER homeostasis, is one of the major triggers of the UPR [72]. Therefore, the data suggest that early-onset hypoxic pregnancy upregulates placental GRP78 in an attempt to re-establish ER homeostasis and resolve ER stress. On the other hand, activation of the PERK-ATF4 pathway may increase oxidative defence mechanisms by facilitating anti-oxidant enzyme expression [73]. Indeed, this hypothesis is supported in the present study in hypoxic pregnancy supplemented by MitoQ. In this instance, the lack of upregulation of ATF4 in response to increased placental GRP78 implies that exogenous MitoQ supplementation renders the activation of placental oxidative defence mechanisms unnecessary. Our data support previous studies in which glucose-regulated proteins (GRPs) have been shown to be induced by hypoxic conditions [74-76]. Severe hypoxia or anoxia has been shown to activate ATF4 [77, 78]. Of interest, both GRP78 and AFT4 protein levels have been shown to be upregulated in the placentae of women with either early- or late-onset preeclampsia [79-81].

The AKT-mTOR signalling pathway plays a crucial role in the regulation of placental size. AKT-mTOR signalling has been shown to be up-regulated in pregnancies from obese women [82], and down-regulated in placentas from growth restricted pregnancies [28]. In relation to hypoxic pregnancy, studies have shown both up- and down-regulation of this pathway, in rodent and human pregnancies [13, 15, 23]. In the present study, placental AKT and p-AKT (Thr308) protein expression remained unchanged despite an increase in

placental volume in hypoxic pregnancy. This suggests that other growth regulatory pathways may be involved, such as the mitogen-activated protein kinase [83].

In the current study there was no evidence of oxidative stress or lipid peroxidation in hypoxic placentae with or without MitoQ treatment. However, the immunostaining of the mitochondrial stress markers GRP75 and TID-1 was found to be increased in the placentae of hypoxic pregnancies, but restored with MitoQ treatment. There is extensive evidence in the literature of studies including our own, for the protection of mitochondrial function *in vivo* by MitoQ treatment in other tissues from various animal models of pathology, including the liver [84], the heart [85], the kidney [86], as well as vascular endothelial cells [66]. Taken together, our data therefore demonstrate that hypoxia induces a low-grade ER and mitochondrial stress by activating the PERK-eIF2α-ATF4 pathway, while treatment of hypoxic pregnancy with MitoQ was effective in suppressing their activation.

MitoQ uptake during pregnancy

In the current study, MitoQ was administered at a dose of 500 μM in the dam's drinking water, from day 6 to day 20 of pregnancy. This equated to approximately 0.044mg MitoQ/g/day. Liquid chromatography-tandem mass spectrometry results indicated that MitoQ uptake by the placenta and maternal liver was considerably greater than that of the fetal liver. The range of tissue concentrations of MitoQ in the placenta (~105pmol/g) and maternal liver (~180pmol/g) is comparable to concentrations that have been demonstrated to protect cells in culture from oxidative damage [87]. Previous studies in which the same dose was administrated to mice in drinking water over several weeks, demonstrated a rapid steady-state distribution of the compound in the heart, liver, kidneys, and skeletal muscle [36]. During pregnancy, MitoQ uptake appears very low in the fetus. This suggests that the potential benefit to the fetus of MitoQ supplementation at this dose during complicated pregnancy is via actions directly on the placenta. These

findings are in keeping with the protective effects of MitoQ on fetal brain development, despite being bound to nanoparticles which prevented transfer of the antioxidant to the fetus [49].

Maternal haematocrit, food and water intake

Hypoxia-inducible factors (HIFs) orchestrate the classical physiological response to systemic hypoxia that results in increased erythropoietin levels and an increase in red blood production [88]. MitoQ in hypoxic pregnancy did not prevent the increase in maternal haematocrit measured in untreated hypoxic pregnancy, suggesting that supplementation with MitoQ does not affect maternal oxygen sensing. In the present study, maternal food and water intake, as well as maternal weight, were transiently affected by maternal treatment with MitoQ in both normoxic and hypoxic pregnancy. This suggests that the pregnant rats possibly had to adapt to the taste of MitoQ. However, in human clinical trials with MitoQ administration, possible taste adversity has been satisfactorily resolved by formulating treatment via a tablet [48, 89].

Future Directions

There is growing evidence for the importance of addressing sex differences in the programming of disease by adverse prenatal conditions. We focussed on the placentae from male offspring, as males appear more sensitive to altered oxygen and supply due to their higher rate of intrauterine growth, relative to females [90]. In the present study we controlled for sex differences, but did not address them. Future studies should examine the sex-specific effects of hypoxic pregnancy, with or without antioxidant treatment, on placenta phenotype.

Although maternal antioxidant therapy was administered from the onset of chronic fetal hypoxia, which may limit translation to the clinic, the data provide proof-of-principle that mitochondria-targeted antioxidants may be beneficial in complicated pregnancy. Clinically, diagnosis of chronic fetal hypoxia would need to be established prior to the induction of maternal antioxidant treatment. Studies in chick embryos have reported that treatment of hypoxic incubations with agents that increase NO bioavailability or antioxidants, such sildenafil or melatonin, can protect against cardiovascular dysfunction in the offspring even when therapy is started 12 days after the induction of chronic hypoxia [91, 92]. The chick embryo may therefore prove a useful model to further assess human translational mitochondrial-targeted antioxidant therapies in pregnancies complicated by hypoxia.

Conclusions

Early-onset hypoxic pregnancy in rodents induces morphological adaptations in the placenta that offset increased placental UPR signalling, aiming to sustain fetal growth. Maternal treatment with the mitochondria-targeted antioxidant MitoQ in hypoxic pregnancy conferred protection against placental UPR activation, mitochondrial stress, and further modified placental morphology by increasing the maternal blood spaces. The data suggest that mitochondria-targeted antioxidants may be beneficial in complicated pregnancies and minimise the detrimental effects on fetal development of reduced oxygen delivery via mechanisms protecting against activation of the placental UPR, thereby enhancing placental perfusion and efficiency.

ACKNOWLEDGEMENTS

We are thankful to the Combined Animal Facility, University of Cambridge, for their excellent technical assistance and help with animal maintenance. DAG is a Professorial Fellow at Gonville & Caius College and a Royal Society Wolfson Research Merit Award Holder.

REFERENCES

1. Sferruzzi-Perri AN, Camm EJ: The Programming Power of the Placenta. Frontiers in physiology 2016, 7:33.

2. Burton GJ, Fowden AL, Thornburg KL: Placental Origins of Chronic Disease. Physiol Rev 2016, 96:1509-65.

3. Dimasuay KG, Boeuf P, Powell TL, Jansson T: Placental Responses to Changes in the Maternal Environment Determine Fetal Growth. Frontiers in physiology 2016, 7:12.

4. Cindrova-Davies T, Herrera EA, Niu Y, Kingdom J, Giussani DA, Burton GJ: Reduced cystathionine gamma-lyase and increased miR-21 expression are associated with increased vascular resistance in growth-restricted pregnancies: hydrogen sulfide as a placental vasodilator. Am J Pathol 2013, 182:1448-58.

5. Giussani DA: The fetal brain sparing response to hypoxia: physiological mechanisms. J Physiol 2016, 594:1215-30.

6. Zhou J, Xiao D, Hu Y, Wang Z, Paradis A, Mata-Greenwood E, Zhang L: Gestational hypoxia induces preeclampsia-like symptoms via heightened endothelin-1 signaling in pregnant rats. Hypertension 2013, 62:599-607.

7. Cuffe JS, Walton SL, Singh RR, Spiers JG, Bielefeldt-Ohmann H, Wilkinson L, Little MH, Moritz KM: Mid- to late term hypoxia in the mouse alters placental morphology, glucocorticoid regulatory pathways and nutrient transporters in a sex-specific manner. J Physiol 2014, 592:3127-41.

8. Giussani DA, Davidge ST: Developmental programming of cardiovascular disease by prenatal hypoxia. J Dev Orig Health Dis 2013, 4:328-37.

9. Camm EJ, Hansell JA, Kane AD, Herrera EA, Lewis C, Wong S, Morrell NW, Giussani DA: Partial contributions of developmental hypoxia and undernutrition to prenatal alterations in somatic growth and cardiovascular structure and function. Am J Obstet Gynecol 2010, 203:495 e24-34.

10. Brain KL, Allison BJ, Niu Y, Cross CM, Itani N, Kane AD, Herrera EA, Giussani DA: Induction of controlled hypoxic pregnancy in large mammalian species. Physiological reports 2015, 3.

11. Richter HG, Camm EJ, Modi BN, Naeem F, Cross CM, Cindrova-Davies T, Spasic-Boskovic O, Dunster C, Mudway IS, Kelly FJ, Burton GJ, Poston L, Giussani DA: Ascorbate prevents placental oxidative stress and enhances birth weight in hypoxic pregnancy in rats. J Physiol 2012, 590:1377-87.

12. Jang EA, Longo LD, Goyal R: Antenatal maternal hypoxia: criterion for fetal growth restriction in rodents. Frontiers in physiology 2015, 6:176.

13. Higgins JS, Vaughan OR, Fernandez de Liger E, Fowden AL, Sferruzzi-Perri AN: Placental phenotype and resource allocation to fetal growth are modified by the timing and degree of hypoxia during mouse pregnancy. J Physiol 2016, 594:1341-56.

14. Rueda-Clausen CF, Stanley JL, Thambiraj DF, Poudel R, Davidge ST, Baker PN: Effect of prenatal hypoxia in transgenic mouse models of preeclampsia and fetal growth restriction. Reprod Sci 2014, 21:492-502.

15. Matheson H, Veerbeek JH, Charnock-Jones DS, Burton GJ, Yung HW: Morphological and molecular changes in the murine placenta exposed to normobaric hypoxia throughout pregnancy. J Physiol 2016, 594:1371-88.

16. Ho-Chen JK, Ain R, Alt AR, Wood JG, Gonzalez NC, Soares MJ: Hypobaric hypoxia as a tool to study pregnancy-dependent responses at the maternal-fetal interface. Methods in molecular medicine 2006, 122:427-34.

17. Rosario GX, Konno T, Soares MJ: Maternal hypoxia activates endovascular trophoblast cell invasion. Dev Biol 2008, 314:362-75.

18. Schwartz JE, Kovach A, Meyer J, McConnell C, Iwamoto HS: Brief, intermittent hypoxia restricts fetal growth in Sprague-Dawley rats. Biol Neonate 1998, 73:313-9.

19. Williams SJ, Campbell ME, McMillen IC, Davidge ST: Differential effects of maternal hypoxia or nutrient restriction on carotid and femoral vascular function in neonatal rats. Am J Physiol Regul Integr Comp Physiol 2005, 288:R360-7.

20. Burton GJ, Jauniaux E: Placental oxidative stress: from miscarriage to preeclampsia. J Soc Gynecol Investig 2004, 11:342-52.

21. Jauniaux E, Poston L, Burton GJ: Placental-related diseases of pregnancy: Involvement of oxidative stress and implications in human evolution. Hum Reprod Update 2006, 12:747-55.

22. Jefferson JA, Simoni J, Escudero E, Hurtado ME, Swenson ER, Wesson DE, Schreiner GF, Schoene RB, Johnson RJ, Hurtado A: Increased oxidative stress following acute and chronic high altitude exposure. High Alt Med Biol 2004, 5:61-9.

23. Yung HW, Cox M, Tissot van Patot M, Burton GJ: Evidence of endoplasmic reticulum stress and protein synthesis inhibition in the placenta of non-native women at high altitude. FASEB J 2012, 26:1970-81.

24. Burton GJ, Yung HW: Endoplasmic reticulum stress in the pathogenesis of early-onset pre-eclampsia. Pregnancy hypertension 2011, 1:72-8.

25. Schroder M, Kaufman RJ: The mammalian unfolded protein response. Annual review of biochemistry 2005, 74:739-89.

26. Ron D, Walter P: Signal integration in the endoplasmic reticulum unfolded protein response. Nat Rev Mol Cell Biol 2007, 8:519-29.

27. Wouters BG, Koritzinsky M: Hypoxia signalling through mTOR and the unfolded protein response in cancer. Nature reviews Cancer 2008, 8:851-64.

28. Yung HW, Calabrese S, Hynx D, Hemmings BA, Cetin I, Charnock-Jones DS, Burton GJ: Evidence of placental translation inhibition and endoplasmic reticulum stress in the etiology of human intrauterine growth restriction. Am J Pathol 2008, 173:451-62.

29. Burton GJ, Yung HW, Cindrova-Davies T, Charnock-Jones DS: Placental endoplasmic reticulum stress and oxidative stress in the pathophysiology of unexplained intrauterine growth restriction and early onset preeclampsia. Placenta 2009, 30 Suppl A:S43-8.

30. Yung HW, Atkinson D, Campion-Smith T, Olovsson M, Charnock-Jones DS, Burton GJ: Differential activation of placental unfolded protein response pathways implies heterogeneity in causation of early- and late-onset pre-eclampsia. J Pathol 2014, 234:262-76.

31. Giussani DA, Camm EJ, Niu Y, Richter HG, Blanco CE, Gottschalk R, Blake EZ, Horder KA, Thakor AS, Hansell JA, Kane AD, Wooding FB, Cross CM, Herrera EA: Developmental programming of cardiovascular dysfunction by prenatal hypoxia and oxidative stress. PLoS One 2012, 7:e31017.

32. Kane AD, Herrera EA, Camm EJ, Giussani DA: Vitamin C prevents intrauterine programming of in vivo cardiovascular dysfunction in the rat. Circulation journal : official journal of the Japanese Circulation Society 2013, 77:2604-11.

33. Poston L, Briley AL, Seed PT, Kelly FJ, Shennan AH: Vitamin C and vitamin E in pregnant women at risk for pre-eclampsia (VIP trial): randomised placebo-controlled trial. Lancet 2006, 367:1145-54.

34. Rahimi R, Nikfar S, Rezaie A, Abdollahi M: A meta-analysis on the efficacy and safety of combined vitamin C and E supplementation in preeclamptic women. Hypertension in pregnancy 2009, 28:417-34.

35. Balaban RS, Nemoto S, Finkel T: Mitochondria, oxidants, and aging. Cell 2005, 120:483-95.

36. Smith RA, Porteous CM, Gane AM, Murphy MP: Delivery of bioactive molecules to mitochondria in vivo. Proc Natl Acad Sci U S A 2003, 100:5407-12.

37. Murphy MP, Smith RA: Targeting antioxidants to mitochondria by conjugation to lipophilic cations. Annual review of pharmacology and toxicology 2007, 47:629-56.

38. Adlam VJ, Harrison JC, Porteous CM, James AM, Smith RA, Murphy MP, Sammut IA: Targeting an antioxidant to mitochondria decreases cardiac ischemia-reperfusion injury. FASEB J 2005, 19:1088-95.

39. Graham D, Huynh NN, Hamilton CA, Beattie E, Smith RA, Cocheme HM, Murphy MP, Dominiczak AF: Mitochondria-targeted antioxidant MitoQ10 improves endothelial function and attenuates cardiac hypertrophy. Hypertension 2009, 54:322-8.

40. Supinski GS, Murphy MP, Callahan LA: MitoQ administration prevents endotoxin-induced cardiac dysfunction. Am J Physiol Regul Integr Comp Physiol 2009, 297:R1095-102.

41. Lowes DA, Thottakam BM, Webster NR, Murphy MP, Galley HF: The mitochondria-targeted antioxidant MitoQ protects against organ damage in a lipopolysaccharide-peptidoglycan model of sepsis. Free Radic Biol Med 2008, 45:1559-65.

42. Chacko BK, Reily C, Srivastava A, Johnson MS, Ye Y, Ulasova E, Agarwal A, Zinn KR, Murphy MP, Kalyanaraman B, Darley-Usmar V: Prevention of diabetic nephropathy in Ins2(+/)(-)(AkitaJ) mice by the mitochondria-targeted therapy MitoQ. Biochem J 2010, 432:9-19.

43. Ghosh A, Chandran K, Kalivendi SV, Joseph J, Antholine WE, Hillard CJ, Kanthasamy A, Kanthasamy A, Kalyanaraman B: Neuroprotection by a mitochondria-targeted drug in a Parkinson's disease model. Free Radic Biol Med 2010, 49:1674-84.

44. Chandran K, Aggarwal D, Migrino RQ, Joseph J, McAllister D, Konorev EA, Antholine WE, Zielonka J, Srinivasan S, Avadhani NG, Kalyanaraman B: Doxorubicin inactivates myocardial cytochrome c oxidase in rats: cardioprotection by Mito-Q. Biophys J 2009, 96:1388-98.

45. McManus MJ, Murphy MP, Franklin JL: The mitochondria-targeted antioxidant MitoQ prevents loss of spatial memory retention and early neuropathology in a transgenic mouse model of Alzheimer's disease. J Neurosci 2011, 31:15703-15.

46. Rodriguez-Cuenca S, Cocheme HM, Logan A, Abakumova I, Prime TA, Rose C, Vidal-Puig A, Smith AC, Rubinsztein DC, Fearnley IM, Jones BA, Pope S, Heales SJ, Lam BY, Neogi SG, McFarlane I, James AM, Smith RA, Murphy MP: Consequences of long-term oral administration of the mitochondria-targeted antioxidant MitoQ to wild-type mice. Free Radic Biol Med 2010, 48:161-72.

47. Smith RA, Murphy MP: Animal and human studies with the mitochondria-targeted antioxidant MitoQ. Ann N Y Acad Sci 2010, 1201:96-103.

48. Snow BJ, Rolfe FL, Lockhart MM, Frampton CM, O'Sullivan JD, Fung V, Smith RA, Murphy MP, Taylor KM, Protect Study G: A double-blind, placebo-controlled study to assess the mitochondria-targeted antioxidant MitoQ as a disease-modifying therapy in Parkinson's disease. Mov Disord 2010, 25:1670-4.

49. Phillips TJ, Scott H, Menassa DA, Bignell AL, Sood A, Morton JS, Akagi T, Azuma K, Rogers MF, Gilmore CE, Inman GJ, Grant S, Chung Y, Aljunaidy MM, Cooke CL, Steinkraus BR, Pocklington A, Logan A, Collett GP, Kemp H, Holmans PA, Murphy MP, Fulga TA, Coney AM, Akashi M, Davidge ST, Case CP: Treating the placenta to prevent adverse effects of gestational hypoxia on fetal brain development. Scientific reports 2017, 7:9079.

50. Richter HG, Hansell JA, Raut S, Giussani DA: Melatonin improves placental efficiency and birth weight and increases the placental expression of antioxidant enzymes in undernourished pregnancy. J Pineal Res 2009, 46:357-64.

51. Camm EJ, Martin-Gronert MS, Wright NL, Hansell JA, Ozanne SE, Giussani DA: Prenatal hypoxia independent of undernutrition promotes molecular markers of insulin resistance in adult offspring. FASEB J 2011, 25:420-7.

52. Pung YF, Rocic P, Murphy MP, Smith RA, Hafemeister J, Ohanyan V, Guarini G, Yin L, Chilian WM: Resolution of mitochondrial oxidative stress rescues coronary collateral growth in Zucker obese fatty rats. Arterioscler Thromb Vasc Biol 2012, 32:325-34.

53. Coan PM, Ferguson-Smith AC, Burton GJ: Developmental dynamics of the definitive mouse placenta assessed by stereology. Biol Reprod 2004, 70:1806-13.

54. Vaughan OR, Sferruzzi-Perri AN, Coan PM, Fowden AL: Adaptations in placental phenotype depend on route and timing of maternal dexamethasone administration in mice. Biol Reprod 2013, 89:80.

55. Gundersen HJ, Osterby R: Optimizing sampling efficiency of stereological studies in biology: or 'do more less well!'. J Microsc 1981, 121:65-73.

56. Mayhew TM: Changes in fetal capillaries during preplacental hypoxia: growth, shape remodelling and villous capillarization in placentae from high-altitude pregnancies. Placenta 2003, 24:191-8.

57. Baddeley AJ, Gundersen HJ, Cruz-Orive LM: Estimation of surface area from vertical sections. J Microsc 1986, 142:259-76.

58. Jensen EB, Gundersen HJ, Osterby R: Determination of membrane thickness distribution from orthogonal intercepts. J Microsc 1979, 115:19-33.

59. Burton GJ, Feneley MR: Capillary volume fraction is the principal determinant of villous membrane thickness in the normal human placenta at term. J Dev Physiol 1992, 17:39-45.

60. Mayhew TM, Joy CF, Haas JD: Structure-function correlation in the human placenta: the morphometric diffusing capacity for oxygen at full term. J Anat 1984, 139 (Pt 4):691-708.

61. Schneider CA, Rasband WS, Eliceiri KW: NIH Image to ImageJ: 25 years of image analysis. Nat Methods 2012, 9:671-5.

62. West BT: Analyzing longitudinal data with the linear mixed models procedure in SPSS. Evaluation & the health professions 2009, 32:207-28.

63. Fonseca BM, Correia-da-Silva G, Teixeira NA: The rat as an animal model for fetoplacental development: a reappraisal of the post-implantation period. Reproductive biology 2012, 12:97-118.

64. Cartwright JE, Keogh RJ, Tissot van Patot MC: Hypoxia and placental remodelling. Adv Exp Med Biol 2007, 618:113-26.

65. Thakor AS, Herrera EA, Seron-Ferre M, Giussani DA: Melatonin and vitamin C increase umbilical blood flow via nitric oxide-dependent mechanisms. J Pineal Res 2010, 49:399-406.

66. Gioscia-Ryan RA, LaRocca TJ, Sindler AL, Zigler MC, Murphy MP, Seals DR: Mitochondria-targeted antioxidant (MitoQ) ameliorates age-related arterial endothelial dysfunction in mice. J Physiol 2014, 592:2549-61.

67. Cooke JP: NO and angiogenesis. Atherosclerosis Supplements 2003, 4:53-60.

68. Yung HW, Colleoni F, Atkinson D, Cook E, Murray AJ, Burton GJ, Charnock-Jones DS: Influence of speed of sample processing on placental energetics and signalling pathways: implications for tissue collection. Placenta 2014, 35:103-8.

69. Cox JS, Shamu CE, Walter P: Transcriptional induction of genes encoding endoplasmic reticulum resident proteins requires a transmembrane protein kinase. Cell 1993, 73:1197-206.

70. Harding HP, Zhang Y, Zeng H, Novoa I, Lu PD, Calfon M, Sadri N, Yun C, Popko B, Paules R, Stojdl DF, Bell JC, Hettmann T, Leiden JM, Ron D: An integrated stress response regulates amino acid metabolism and resistance to oxidative stress. Mol Cell 2003, 11:619-33.

71. Chandel NS, Maltepe E, Goldwasser E, Mathieu CE, Simon MC, Schumacker PT: Mitochondrial reactive oxygen species trigger hypoxia-induced transcription. Proc Natl Acad Sci U S A 1998, 95:11715-20.

72. Xu C, Bailly-Maitre B, Reed JC: Endoplasmic reticulum stress: cell life and death decisions. J Clin Invest 2005, 115:2656-64.

73. Cullinan SB, Diehl JA: Coordination of ER and oxidative stress signaling: the PERK/Nrf2 signaling pathway. Int J Biochem Cell Biol 2006, 38:317-32.

74. Ozawa K, Kuwabara K, Tamatani M, Takatsuji K, Tsukamoto Y, Kaneda S, Yanagi H, Stern DM, Eguchi Y, Tsujimoto Y, Ogawa S, Tohyama M: 150-kDa oxygen-regulated protein (ORP150) suppresses hypoxia-induced apoptotic cell death. J Biol Chem 1999, 274:6397-404.

75. Ozawa K, Kondo T, Hori O, Kitao Y, Stern DM, Eisenmenger W, Ogawa S, Ohshima T: Expression of the oxygen-regulated protein ORP150 accelerates wound healing by modulating intracellular VEGF transport. J Clin Invest 2001, 108:41-50.

76. Heacock CS, Sutherland RM: Enhanced synthesis of stress proteins caused by hypoxia and relation to altered cell growth and metabolism. Br J Cancer 1990, 62:217-25.

77. Blais JD, Filipenko V, Bi M, Harding HP, Ron D, Koumenis C, Wouters BG, Bell JC: Activating transcription factor 4 is translationally regulated by hypoxic stress. Mol Cell Biol 2004, 24:7469-82.

78. Estes SD, Stoler DL, Anderson GR: Normal fibroblasts induce the C/EBP beta and ATF-4 bZIP transcription factors in response to anoxia. Exp Cell Res 1995, 220:47-54.

79. Du L, He F, Kuang L, Tang W, Li Y, Chen D: eNOS/iNOS and endoplasmic reticulum stress-induced apoptosis in the placentas of patients with preeclampsia. J Hum Hypertens 2017, 31:49-55.

80. Fu J, Zhao L, Wang L, Zhu X: Expression of markers of endoplasmic reticulum stress-induced apoptosis in the placenta of women with early and late onset severe pre-eclampsia. Taiwan J Obstet Gynecol 2015, 54:19-23.

81. Mizuuchi M, Cindrova-Davies T, Olovsson M, Charnock-Jones DS, Burton GJ, Yung HW: Placental endoplasmic reticulum stress negatively regulates transcription of placental growth factor via ATF4 and ATF6beta: implications for the pathophysiology of human pregnancy complications. J Pathol 2016, 238:550-61.

82. Jansson N, Rosario FJ, Gaccioli F, Lager S, Jones HN, Roos S, Jansson T, Powell TL: Activation of placental mTOR signaling and amino acid transporters in obese women giving birth to large babies. J Clin Endocrinol Metab 2013, 98:105-13.

83. Hatano N, Mori Y, Oh-hora M, Kosugi A, Fujikawa T, Nakai N, Niwa H, Miyazaki J, Hamaoka T, Ogata M: Essential role for ERK2 mitogen-activated protein kinase in placental development. Genes Cells 2003, 8:847-56.

84. Rehman H, Liu Q, Krishnasamy Y, Shi Z, Ramshesh VK, Haque K, Schnellmann RG, Murphy MP, Lemasters JJ, Rockey DC, Zhong Z: The mitochondria-targeted antioxidant MitoQ attenuates liver fibrosis in mice. International journal of physiology, pathophysiology and pharmacology 2016, 8:14-27.

85. Dare AJ, Logan A, Prime TA, Rogatti S, Goddard M, Bolton EM, Bradley JA, Pettigrew GJ, Murphy MP, Saeb-Parsy K: The mitochondria-targeted anti-oxidant MitoQ decreases ischemia-reperfusion injury in a murine syngeneic heart transplant model. J Heart Lung Transplant 2015, 34:1471-80.

86. Dare AJ, Bolton EA, Pettigrew GJ, Bradley JA, Saeb-Parsy K, Murphy MP: Protection against renal ischemia-reperfusion injury in vivo by the mitochondria targeted antioxidant MitoQ. Redox biology 2015, 5:163-8.

87. Jauslin ML, Meier T, Smith RA, Murphy MP: Mitochondria-targeted antioxidants protect Friedreich Ataxia fibroblasts from endogenous oxidative stress more effectively than untargeted antioxidants. FASEB J 2003, 17:1972-4.

88. Haase VH: Regulation of erythropoiesis by hypoxia-inducible factors. Blood reviews 2013, 27:41-53.

89. Gane EJ, Weilert F, Orr DW, Keogh GF, Gibson M, Lockhart MM, Frampton CM, Taylor KM, Smith RA, Murphy MP: The mitochondria-targeted anti-oxidant mitoquinone decreases liver damage in a phase II study of hepatitis C patients. Liver international : official journal of the International Association for the Study of the Liver 2010, 30:1019-26.

90. Clifton VL: Review: Sex and the human placenta: mediating differential strategies of fetal growth and survival. Placenta 2010, 31 Suppl:S33-9.

91. Itani N, Skeffington KL, Beck C, Niu Y, Giussani DA: Melatonin rescues cardiovascular dysfunction during hypoxic development in the chick embryo. J Pineal Res 2016, 60:16-26.

92. Itani N, Skeffington KL, Beck C, Giussani DA: Sildenafil therapy for fetal cardiovascular dysfunction during hypoxic development: studies in the chick embryo. J Physiol 2017, 595:1563-73.

Table 1. Maternal biometric data. Haematocrit, body weight (BW), crown-rump length (CRL), head diameter (HD), body mass index (BMI), HD:BW from normoxic (N), hypoxic (H), hypoxic+MitoQ (HM) and normoxic+MitoQ (NM) dams at day 20 of gestation. Values are mean±S.E.M. * indicates significant main effect of hypoxia on haematocrit, $p<0.05$, General Linear Model test. Number of dams for Hct: N=16; H=16; HM=18; NM=16. Number of dams for remaining variables: N=10; H=10; HM=11; NM=11.

	N	**H**	**HM**	**NM**
Haematocrit (%)	34.7 ±1.9	40.9±1.5*	39.9±1.2*	37.9±0.6
BW (g)	410.2±7.2	395.6±8.6	387.4±10.4	391.4±8.7
CRL (mm)	190.7±2.0	187.2±3.0	199.6±6.1	184.5±4.1
HD (mm)	22.8±0.5	22.7±0.5	22.5±0.3	23.2±0.3
BMI	11.3±0.3	11.4±0.5	10.0±0.6	11.6±0.5
HD:BW	0.056±0.001	0.058±0.002	0.059±0.002	0.059±0.002

Table 2. Fetal Biometric Data. Body weight (BW), placental weight (PW), placental efficiency (BW:PW), crown-rump length (CRL), head diameter (HD), body mass index (BMI) and HD:BW from male fetuses only from normoxic (N), hypoxic (H) , hypoxic+MitoQ (HM) and normoxic+MitoQ (NM) pregnancy at day 20 of gestation. Values are mean±S.E.M. *indicates significant main effect of hypoxia on placental weight, $p<0.05$, Mixed Linear Model test**.** Number of fetuses for BW: N=74; H=86; HM=84; NM=65. Number of fetuses for remaining variables: N=59; H=59; HM=62; NM=54.

	N	**H**	**HM**	**NM**
BW (g)	3.63±0.05	3.41±0.03	3.72±0.06	3.39±0.04
PW (g)	0.55±0.01	0.62±0.01*	0.60±0.01*	0.54±0.01
BW:PW	6.69±0.15	5.77±0.15	6.44±0.18	6.49±0.15
CRL (mm)	33.19±0.30	32.23±0.30	33.12±0.24	32.35±0.31
HD (mm)	7.73±0.07	7.72±0.06	7.78±0.07	7.60±0.06
BMI index	3.33±0.04	3.38±0.08	3.43±0.04	3.32±0.05
HD:BW	2.14±0.03	2.25±0.03	2.09±0.04	2.25±0.03

FIGURES

Figure 1. Effects of maternal hypoxia with or without MitoQ treatment on maternal parameters during days 6 to 20 of gestation. Values are mean±S.E.M. (A) maternal water intake expressed relative to body weight, (B) maternal food intake expressed relative to body weight, and (C) maternal body weight in normoxic (N), hypoxic (H), hypoxic+MitoQ (HM) and normoxic+MitoQ (NM) pregnancies. * *vs.* N, $p<0.05$, † *vs.* H, ‡ *vs*. NM, General Linear Model repeated measures test.

Figure 2. Effects of maternal hypoxia with or without MitoQ treatment on placental volumes at day 20 of gestation. Values are mean±S.E.M. (A) Total placental volume and (B) compartmental volumes, in normoxic (N), hypoxic (H), hypoxic+MitoQ (HM) and normoxic+MitoQ (NM) pregnancies. * *vs.* N, ‡ *vs*. NM, $p<0.05$, General Linear Model test. A representative haematoxylin and eosin-stained paraffin section of the placenta is shown for each group. Abbreviations: DB= decidua basalis, JZ= junctional zone, LZ= labyrinthine zone. Scale bar=1mm.

Figure 3. Effects of maternal hypoxia with or without maternal MitoQ treatment on the volume and surface area of fetal capillaries (FC) and maternal blood spaces (MBC) at day 20 of gestation. Values are mean±S.E.M. (A-B) FC absolute volume and surface area and (C-D) MBS absolute volume and surface area in normoxic (N), hypoxic (H), hypoxic+MitoQ (HM) and normoxic+MitoQ (NM) pregnancies. * *vs.* N, ‡ *vs*. NM, $p<0.05$, General Linear Model test. A representative toluidine blue-stained resin section of the labyrinthine zone is shown from one placentae per group. Abbreviations: FC, fetal capillary; MBS, maternal blood space; T, trophoblast. Scale bar=50µm.

Figure 4. Effects of maternal hypoxia with or without maternal MitoQ treatment on placental efficiency at day 20 of gestation. Values are mean±S.E.M. Fetal body weight (FW) expressed relative to fetal capillary (FC) and maternal blood space (MBC) areas in normoxic (N), hypoxic (H), hypoxic+MitoQ (HM) and normoxic+MitoQ (NM) pregnancies. * *vs.* N, $p<0.05$, General Linear Model test.

Figure 5. Effects of maternal hypoxia with or without maternal MitoQ treatment on barrier thickness, theoretical diffusion capacity (TDC) and specific diffusion capacity (SDC) of the placental interhaemal membrane at day 20 of gestation. Values are mean±S.E.M. (A) Barrier thickness, (B) TDC and (C) SDC in normoxic (N), hypoxic (H), hypoxic+MitoQ (HM) and normoxic+MitoQ (NM) pregnancies.

Figure 6. Effects of maternal hypoxia with or without maternal MitoQ treatment on endoplasmic reticulum (ER) stress signalling pathway at day 20 of gestation. Values are mean±S.E.M. Representative Western blots and mean densitometry for (A) glucose-regulated protein 78 (GRP78) and (B) activating transcription Factor 4 (ATF4) in normoxic (N), hypoxic (H), hypoxic+MitoQ (HM) and normoxic+MitoQ (NM) placentae. After normalization to β-actin, the mean density of the samples was expressed relative to normoxic placentae, assigned an arbitrary value of 1. * *vs.* N, ‡ *vs*. NM, § *vs.* HM, $p<0.05$, General Linear Model test. Representative sections show the localisation of GRP78 and AFT4 in the labyrinthine and junctional zones of the placenta. Abbreviations: DB= decidua basalis, JZ= junctional zone, LZ= labyrinthine zone. Scale bar (placenta)=1mm, scale bar (JZ, LZ)=50µm.

Figure 7. Effects of maternal hypoxia with or without maternal MitoQ treatment on oxidative stress and lipid-peroxidation markers at day 20 of gestation. Values are mean±S.E.M. Representative Western blots and mean densitometry for (A) protein kinase B (AKT), (B) AKT phosphorylation at Thr308 residues (p-AKT Thr 308), (C) 70kDa heat-shock protein (HSP70) and (D) 4-Hydroxynonenal (4-HNE) in normoxic (N),

hypoxic (H), hypoxic+MitoQ (HM) and normoxic+MitoQ (NM) placentae. After normalization to β-actin, the mean density of the samples was expressed relative to normoxic placentae, assigned an arbitrary value of 1.

Figure 8. Effects of maternal hypoxia with or without maternal MitoQ treatment on mitochondrial stress at day 20 of gestation. Values are mean±S.E.M. The mean optical density (O.D.) of (A) glucose-regulated protein 75 (GRP75) and (B) tumorous imaginal disc 1 (TID-1) staining in normoxic (N), hypoxic (H), hypoxic+MitoQ (HM) and normoxic+MitoQ (NM) placentae. Representative sections showing the intensity of GRP75 and TID-1 staining in the labyrinthine zone of the placenta. * *vs.* N, ‡ *vs*. NM, § *vs.* HM, $p<0.05$, General Linear Model test. Scale bar=100µm.

Figure 1.

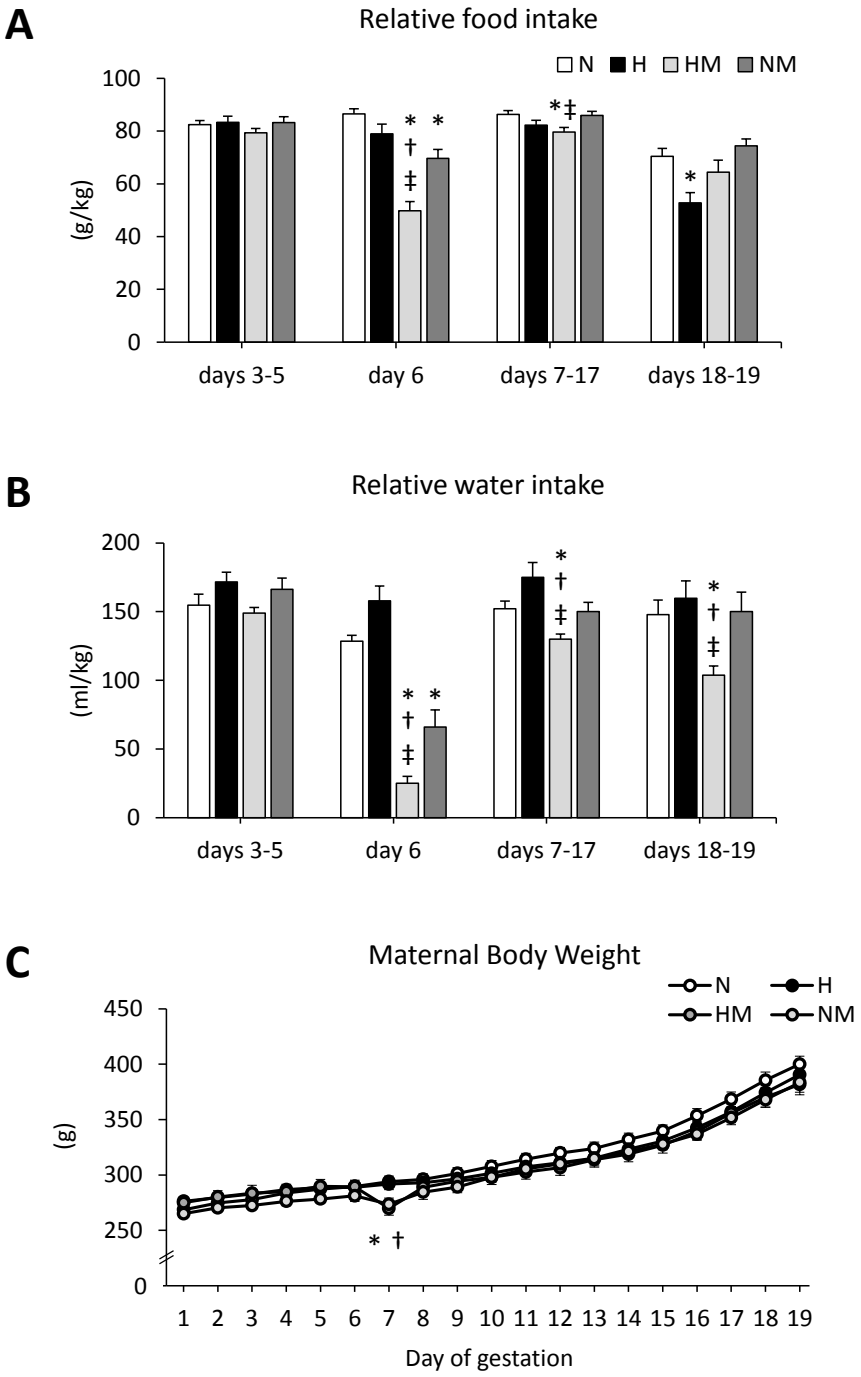
A
Relative food intake
N H HM NM
100
80
60
40
20
0
(g/kg)
days 3-5
day 6
days 7-17
days 18-19
B
Relative water intake
200
150
100
50
0
(ml/kg)
days 3-5
day 6
days 7-17
days 18-19
C
Maternal Body Weight
N H
HM NM
450
400
350
300
250
0
(g)
1 2 3 4 5 6 7 8 9 10 11 12 13 14 15 16 17 18 19
Day of gestation

Figure 2.

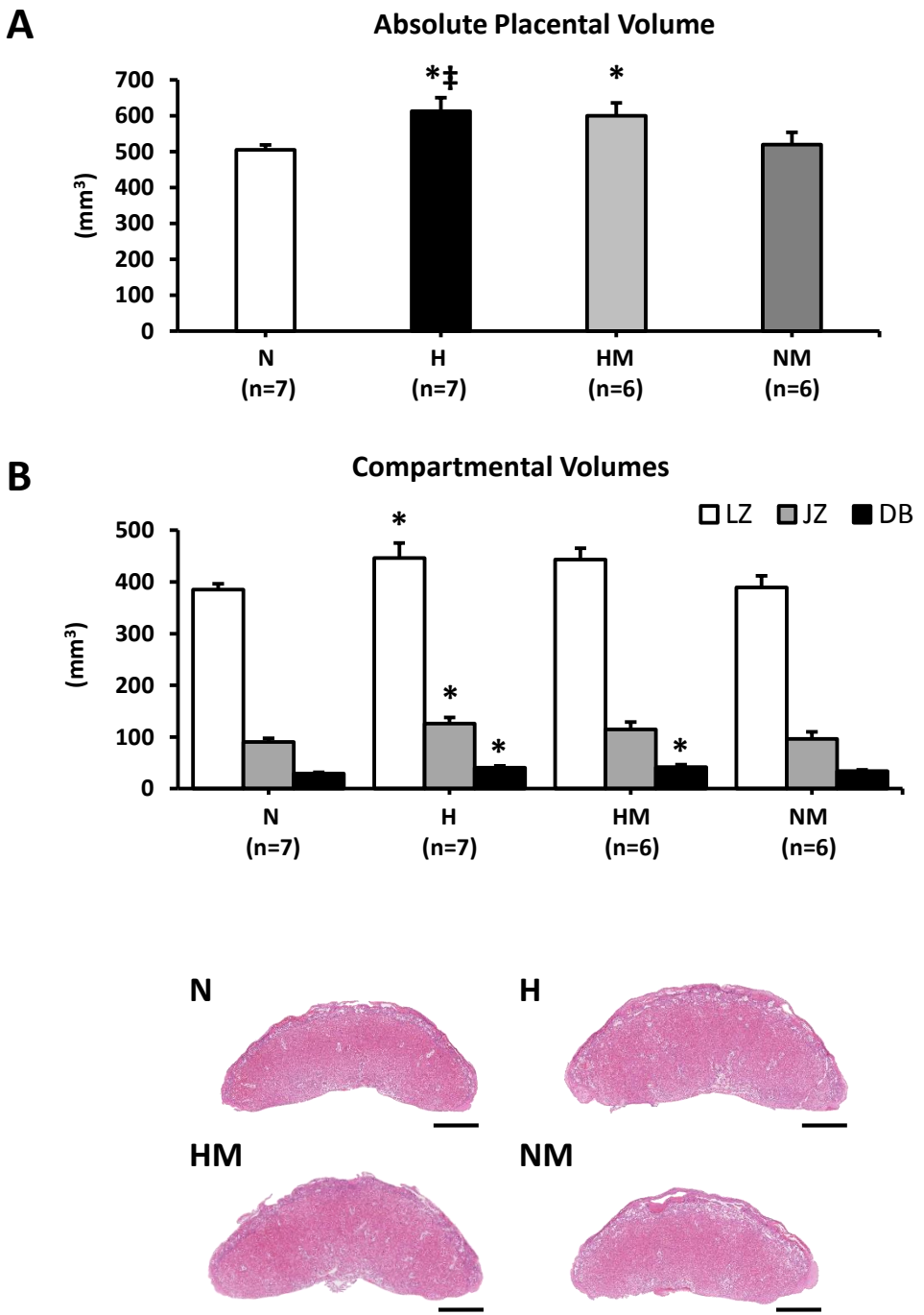
A
Absolute Placental Volume
(mm³)
700
600
500
400
300
200
100
0
*‡
*
N (n=7)
H (n=7)
HM (n=6)
NM (n=6)
B
Compartmental Volumes
LZ
JZ
DB
(mm³)
500
400
300
200
100
0
*
*
*
*
N (n=7)
H (n=7)
HM (n=6)
NM (n=6)
N
H
HM
NM

Figure 3.

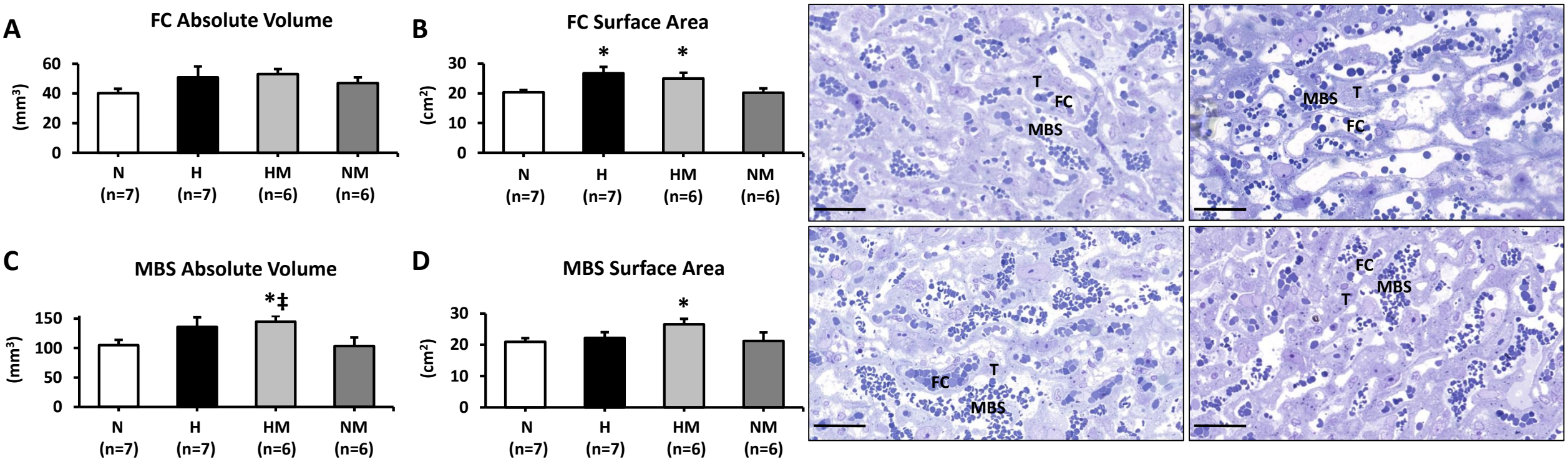
A
FC Absolute Volume
(mm³)
60
40
20
0
N (n=7)
H (n=7)
HM (n=6)
NM (n=6)
B
FC Surface Area
(cm²)
30
20
10
0
*
*
N (n=7)
H (n=7)
HM (n=6)
NM (n=6)
C
MBS Absolute Volume
(mm³)
150
100
50
0
*‡
N (n=7)
H (n=7)
HM (n=6)
NM (n=6)
D
MBS Surface Area
(cm²)
30
20
10
0
*
N (n=7)
H (n=7)
HM (n=6)
NM (n=6)
T
FC
MBS
MBS
T
FC
FC
T
MBS
FC
MBS
T

Figure 5.

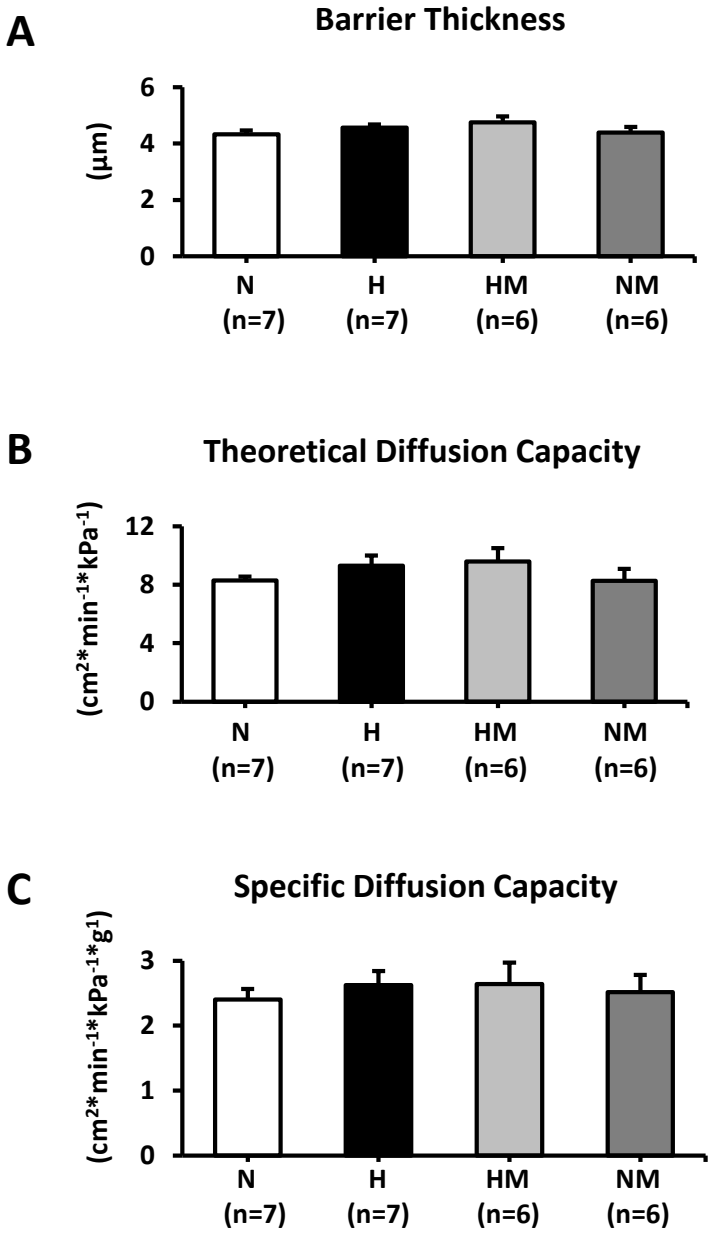
A
Barrier Thickness
(µm)
6
4
2
0
N
(n=7)
H
(n=7)
HM
(n=6)
NM
(n=6)
B
Theoretical Diffusion Capacity
(cm²*min⁻¹*kPa⁻¹)
12
8
4
0
N
(n=7)
H
(n=7)
HM
(n=6)
NM
(n=6)
C
Specific Diffusion Capacity
(cm²*min⁻¹*kPa⁻¹*g¹)
3
2
1
0
N
(n=7)
H
(n=7)
HM
(n=6)
NM
(n=6)

Figure 4.

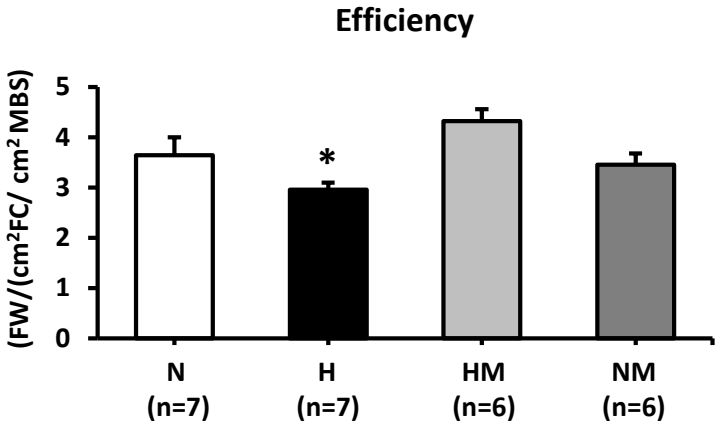

Figure 6.

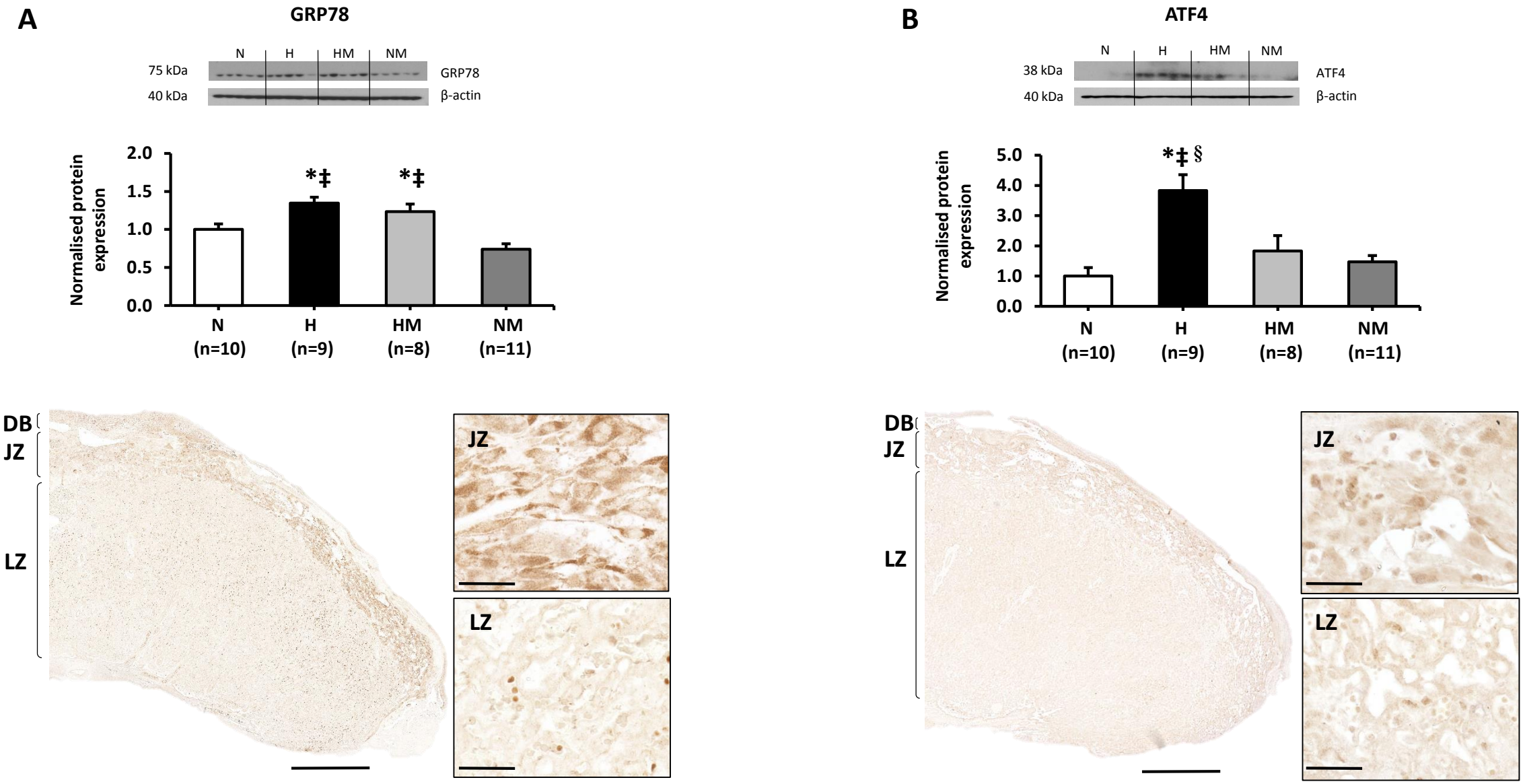
A
GRP78
N
H
HM
NM
75 kDa
40 kDa
GRP78
β-actin
Normalised protein expression
2.0
1.5
1.0
0.5
0.0
*‡
*‡
N (n=10)
H (n=9)
HM (n=8)
NM (n=11)
DB
JZ
LZ
JZ
LZ
B
ATF4
N
H
HM
NM
38 kDa
40 kDa
ATF4
β-actin
Normalised protein expression
5.0
4.0
3.0
2.0
1.0
0.0
*‡ §
N (n=10)
H (n=9)
HM (n=8)
NM (n=11)
DB
JZ
LZ
JZ
LZ

Figure 7.

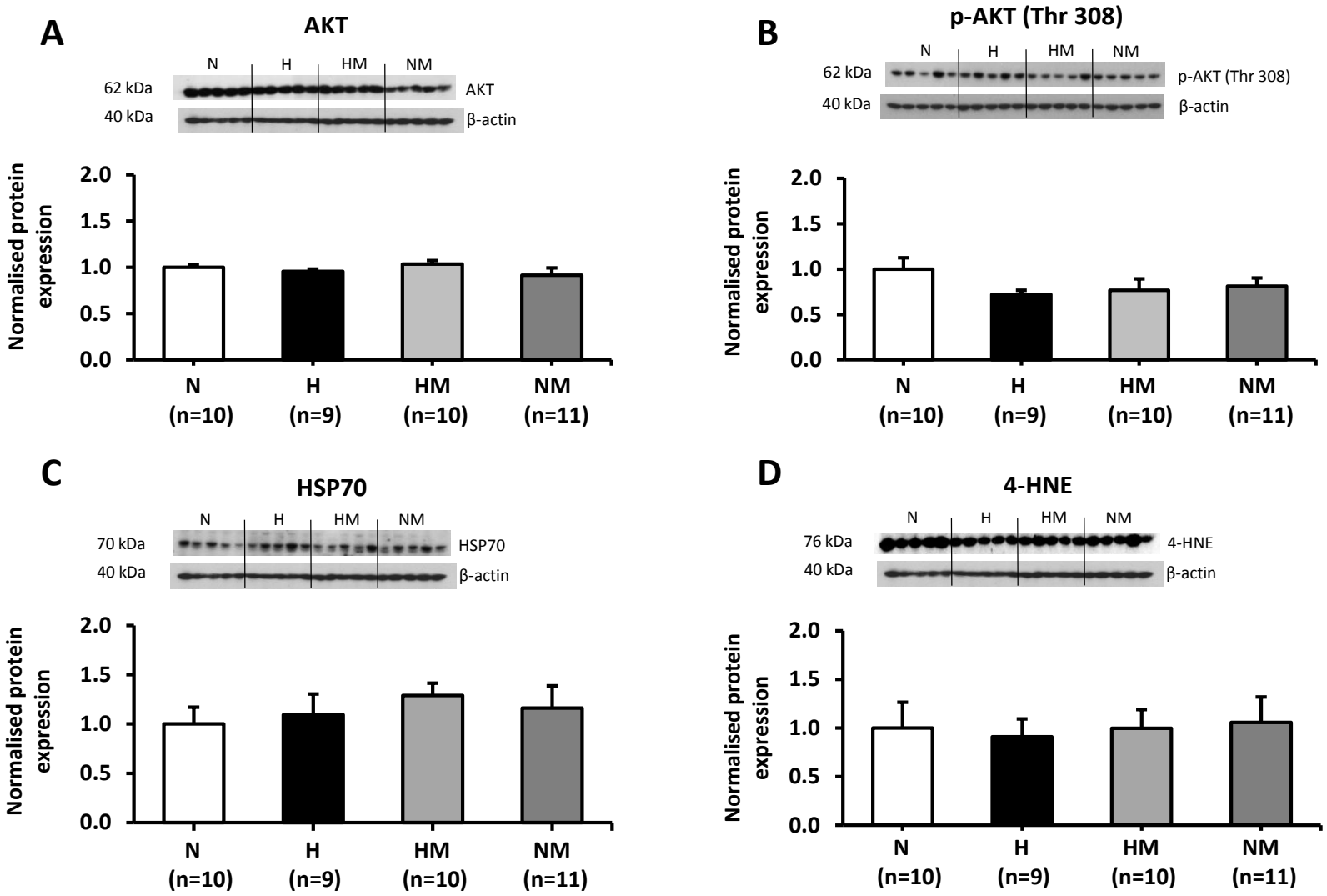
A
AKT
N
H
HM
NM
62 kDa
AKT
40 kDa
β-actin
Normalised protein expression
2.0
1.5
1.0
0.5
0.0
N (n=10)
H (n=9)
HM (n=10)
NM (n=11)
B
p-AKT (Thr 308)
62 kDa
p-AKT (Thr 308)
40 kDa
β-actin
C
HSP70
70 kDa
HSP70
40 kDa
β-actin
D
4-HNE
76 kDa
4-HNE
40 kDa
β-actin

Figure 8.

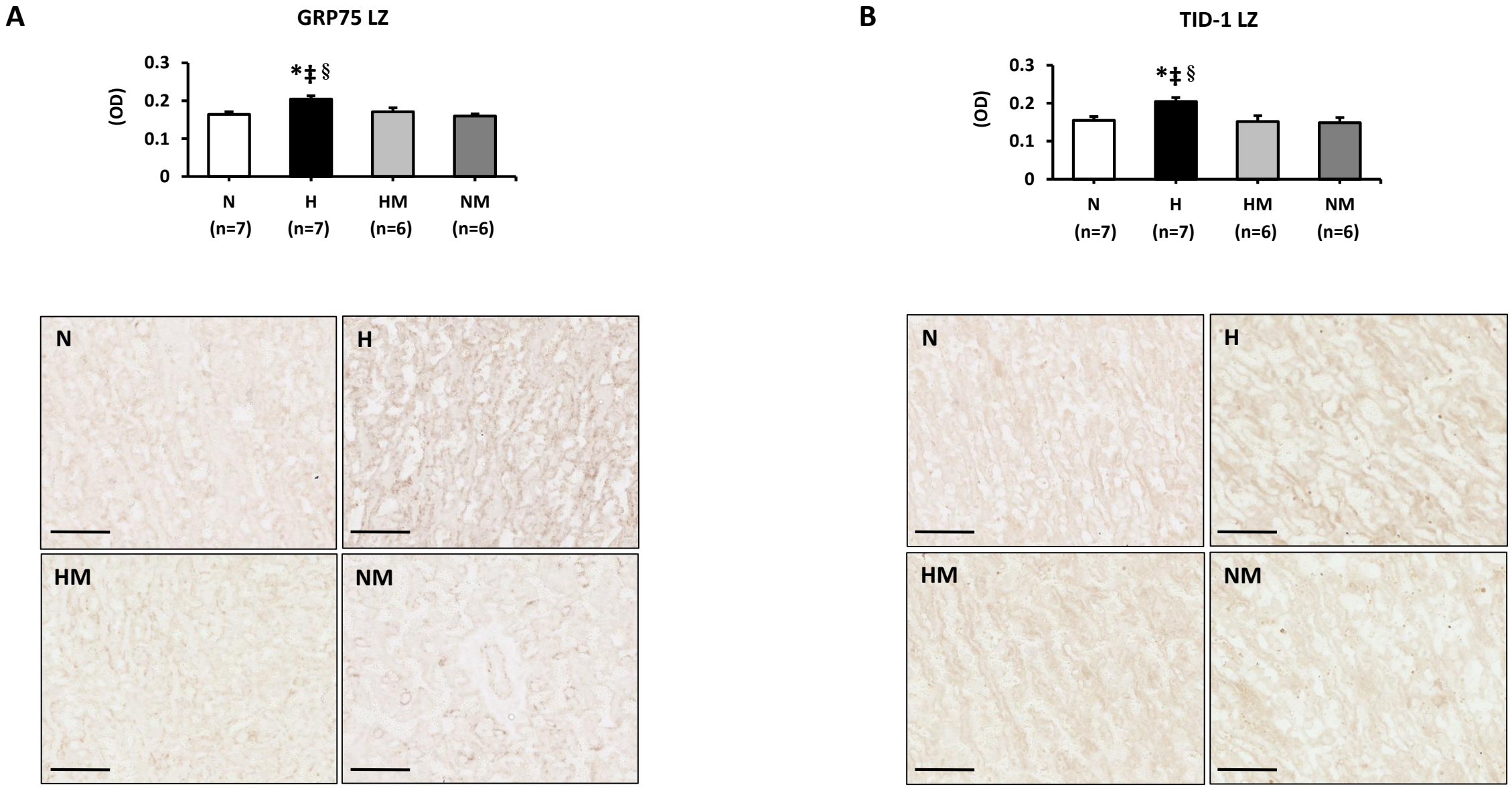
A
GRP75 LZ
0.3
0.2
0.1
0
(OD)
*‡§
N (n=7)
H (n=7)
HM (n=6)
NM (n=6)
B
TID-1 LZ
0.3
0.2
0.1
0
(OD)
*‡§
N (n=7)
H (n=7)
HM (n=6)
NM (n=6)
N
H
HM
NM
N
H
HM
NM